Optimal Diversity-Multiplexing Tradeoff With Group Detection for MIMO Systems

Sana Sfar, *Associate Member, IEEE*, Lin Dai, *Member, IEEE*, and Khaled B. Letaief, *Fellow, IEEE*

***Abstract*—It is well known that multiple-input multiple-output (MIMO) systems provide two types of gains: *diversity* gains and *spatial multiplexing* gains. Recently, a tradeoff function of these two gains has been derived for a point-to-point MIMO system when optimal detection is used. In this paper, we extend the previous work to a more general MIMO system, where the transmitted data is coded in groups. Group detection is applied at the receiver to retrieve the data. It consists of a zero-forcing decorrelation that separates the groups, followed by a joint detection for each of the groups. Two receiver structures are considered in this paper; namely, group zero forcing (GZF) and group successive interference cancellation (GSIC). We assess the *diversity-multiplexing tradeoff* function of each of these receivers over a richly scattered Rayleigh fading channel. Three rate-allocation algorithms will be considered here; namely, equal rate, group-size proportional rate, and optimal-rate allocation. An explicit expression of the system tradeoff will be derived for both receivers with these three rate allocations. The obtained results will first be optimized over all possible group partitions for a given number of groups. Next, the number of groups will be varied to further optimize the system-tradeoff performance. An overall optimum tradeoff for a general MIMO system with group detection will then be obtained. Numerical results will indicate that optimum performance can be approached with very-low-complexity schemes for a wide range of data rates. It will be also demonstrated that group detection bridges the gap between the traditional decorrelator and the optimal receiver tradeoff performances.**

***Index Terms*—Channel capacity, channel multivariate statistics distribution, diversity-multiplexing tradeoff, group detection, multiple-input multiple-output (MIMO) systems, rate allocation.**

I. Introduction

MULTIPLE-INPUT multiple-output (MIMO) systems have been shown to provide significant performance gains over traditional single-antenna systems [1]. These gains fall into two categories; namely, *diversity* and *spatial multiplexing* [2]. Most of the previously designed MIMO systems have focused on the maximization of either type of gain, and have been categorized as either diversity— type systems or high-(data)-rate ones. For example, space–time codes (STCs) [3] and orthogonal designs (ODs) [4], [5] are regarded as diversity-type schemes, and Vertical Bell Layered Space–Time (V-BLAST) schemes [6], [7] as data-rate ones. By exclusively maximizing one type of gain, these schemes unfortunately sacrifice the other type, such as the system capacity with STC [2], [8], [9], and diversity with V-BLAST [2]. Recently, group detection was shown to play a key role in designing schemes that achieve higher diversity gains and data rates than the previously mentioned ones. Proposed systems in [10] and [11] are some examples. In these schemes, signals are arranged in groups and each group is allocated one STC/OD component code [10], [11]. The overall data rate is also shared between these groups, as in V-BLAST. By doing so, group detection allows the proper integration of the diversity-type schemes with high-data-rates ones. A fair comparison of all of these schemes and how much performance improvement group detection provides is obviously of fundamental importance, and is yet an open problem.

Recently and in contrast to common conclusions, [2] has demonstrated that diversity gains and spatial-multiplexing gains are not exclusive. They can still be achieved at the same time with a fundamental tradeoff function that determines the amount of these gains. In particular, the overall performance of any scheme can be assessed according to a unified measure, the tradeoff function, and a fair comparison of different schemes is then possible. The case of OD as well as V-BLAST have both already been treated as examples in [2] in a point-to-point communication context. However, existent studies fall short of the derivation of the tradeoff performance achieved with group detection. Such performance is important not only to determine how much gain group detection can provide, but also to serve as comparison benchmark for any system using group detection [10], [11]. Hence, this paper will evaluate the optimal diversity-multiplexing tradeoff achieved with group detection over a richly scattered Rayleigh-fading narrowband-MIMO channel.

We consider two receiver structures for group detection; namely, group zero forcing (GZF) and group successive interference cancellation (GSIC). With the first receiver, a zero-forcing decorrelator is used to separate the various groups of data. Maximum-likelihood (ML) detection is next simultaneously applied to jointly detect each group of data. As for the second receiver, groups are detected successively in stages. At each stage, one group is detected using ML after canceling the interference of the already detected groups in previous stages. This paper will evaluate the diversity-multiplexing tradeoff functions of these two receivers. We shall note here that when the number of groups is reduced to one, both GZF and GSIC become equivalent to a traditional ML receiver. In addition, when each transmitted signal is regarded as one group by itself, both receivers become equivalent to a traditional decorrelator. The tradeoff functions in these two particular cases have been

Paper approved by D. I. Kim, the Editor for Spread Spectrum Transmission and Access of the IEEE Communications Society. Manuscript received May 28, 2004; revised December 16, 2004. This work was supported in part by the Hong Kong Telecom Institute of Information Technology and in part by the Hong Kong Research Grant Council.

The authors are with Center for Wireless Information Technology, Electrical and Electronic Engineering Department, The Hong Kong University of Science and Technology, Kowloon 190, Hong Kong (e-mail: eesana@ust.hk; eedailin@ust.hk; eekhaled@ee.ust.hk).

Digital Object Identifier 10.1109/TCOMM.2005.851596

already evaluated in [2]. In this paper and in contrast to previous work, we deal with the evaluation of the system-tradeoff performance for a general number of groups. To do so, we first derive the exact distribution of each of the group's outage probability. The latter is defined as the probability that a group does not meet its required allocated data rate. We will then deduce the diversity-multiplexing tradeoff performance function for each of the active groups. It is then demonstrated that the overall system performance is limited by the worst group performance. We will also show that it depends on the number of groups, the group partition in use, and the rate allocated to each of the groups.

Three rate-allocation algorithms are considered throughout this paper; namely, the equal rate, the group-size proportional rate, and the optimal-rate allocation. The first allocation consists of equally splitting the total rate among all the groups. The second one enables groups to transmit with rates that are proportional to the number of signals that they regroup. Finally, the optimal algorithm consists of allocating different rates to different groups with an objective function that maximizes the overall system-tradeoff performance. Both GZF and GSIC tradeoff functions are then explicitly evaluated according to these three rate-allocations schemes. Results will indicate that the group-size proportional allocation scheme outperforms by far the equal-rate one. Moreover, it will be shown that it approaches the optimal allocation performance at high values of multiplexing rates.

As mentioned earlier, the system-tradeoff performance depends on the number of groups, as well as the group partition. Hence, in a first step, we will fix the number of groups to G, and vary the group partition so as to optimize the overall tradeoff obtained earlier with the three rate-allocation algorithms. Significant diversity gains are demonstrated with such an optimization. Particularly, it will be shown that the GZF tradeoff outperforms the GSIC one for some multiplexing rates, in contrast to most of the existent traditional performance comparison results. As a result, receiver designs that aim to reduce the computational complexity will benefit tremendously from the obtained results. Finally, the number of groups G is varied, and the previously derived performance functions are assessed accordingly. It is found that the system-tradeoff performance is further optimized when G is smaller. Results will also demonstrate that group detection bridges the performance gap between the traditional decorrelator and the optimal receiver effectively [2].

This paper is organized as follows. Section II describes the adopted system model, as well as the different notations used throughout the paper. In Section III, the overall system tradeoff is evaluated as a function of the tradeoff of each group. The latter will be fully evaluated in Section IV. In Section V, different rate-allocation schemes are considered, and the overall system-tradeoff function is derived for each. Simulations results are provided in Section VI, and our conclusions are given in Section VII.

II. System Model and Group Detection

We consider a richly scattered, multiple-access, Rayleigh-fading channel with K active antennas transmitting K different signals, and N receive antennas, as shown in Fig. 1. The channel

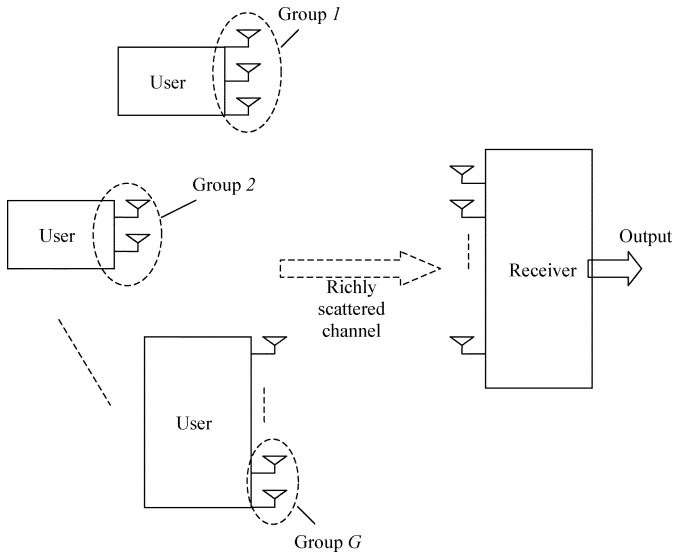

Fig. 1. General system block diagram.

matrix is written as an $N \times K$ matrix $\boldsymbol{H}$, is assumed to be known at the receiver side only, and remains constant within a block of ℓ symbols. The entries of $\boldsymbol{H}$ are assumed to be independent complex circularly symmetric Gaussian distributed with unit variance.

The K transmit antennas are randomly partitioned into G groups, and data is encoded over these G blocks, each of which fades independently. Let $\{p, G\}$ denote a random partition, and denote by $|g^{\{p,G\}}|$ the size of its gth group, such that $K = \sum_{g=1}^{G} |g^{\{p,G\}}|$. $\{p, G\}$ is fully specified by the number of groups G, and the size of each of the groups $|g^{\{p,G\}}|$. To simplify the notations, we will drop the index "$^{\{p,G\}}$" throughout this paper, and shortly denote by "g" the gth group of $\{p, G\}$.

Throughout this paper, we denote by $\boldsymbol{X}$ the transmitted $K \times \ell$ matrix. $\boldsymbol{X}$ is chosen from the codebook C of rate R b/s/Hz. The latter has $\lfloor 2^{R\ell} \rfloor$ $K \times \ell$ matrix codeword matrices, denoted as $\{\boldsymbol{X}(1), \ldots, \boldsymbol{X}(\lfloor 2^{R\ell} \rfloor)\}$. Similar to [2], we consider schemes that support data rates that increase with the average signal-to-noise ratio (SNR) per receive antenna. We will also think of a scheme as a family of codes $\{C(\text{SNR})\}$ of block length ℓ, one on each SNR level, and we shall let $R(\text{SNR})$ denote the overall rate associated with the code $C(\text{SNR})$.

According to the group partition, $\boldsymbol{X}$ can be written as $\boldsymbol{X} = [\boldsymbol{X}_1^T, \boldsymbol{X}_2^T, \ldots, \boldsymbol{X}_G^T]^T$, where $\boldsymbol{X}_g$ is the $|g| \times \ell$ transmitted matrix associated with the gth group. Each $\boldsymbol{X}_g$ will be associated with a data rate $R_g(\text{SNR})$, assigned for the gth group, such that $R(\text{SNR}) = \Sigma_{g=1}^{G} R_g(\text{SNR})$. Finally, $\boldsymbol{X}$ is assumed normalized, so that the average transmit power at each transmit antenna in each symbol period is 1.

Assuming perfect symbol synchronization at the receiver, a discrete model of the $N \times \ell$ received complex signal vector can then be written as

$$\boldsymbol{Y} = \sqrt{\frac{\text{SNR}}{K}} \boldsymbol{H}\boldsymbol{X} + \boldsymbol{V} \tag{1}$$

where $\boldsymbol{V}$ is $\mathcal{N}(\boldsymbol{0}, \boldsymbol{I}_{\mathbf{N}\times\mathbf{N}})$ distributed. When $N \geq K$, $\boldsymbol{H}$ is of full rank K, and group detection is applicable. Considering a

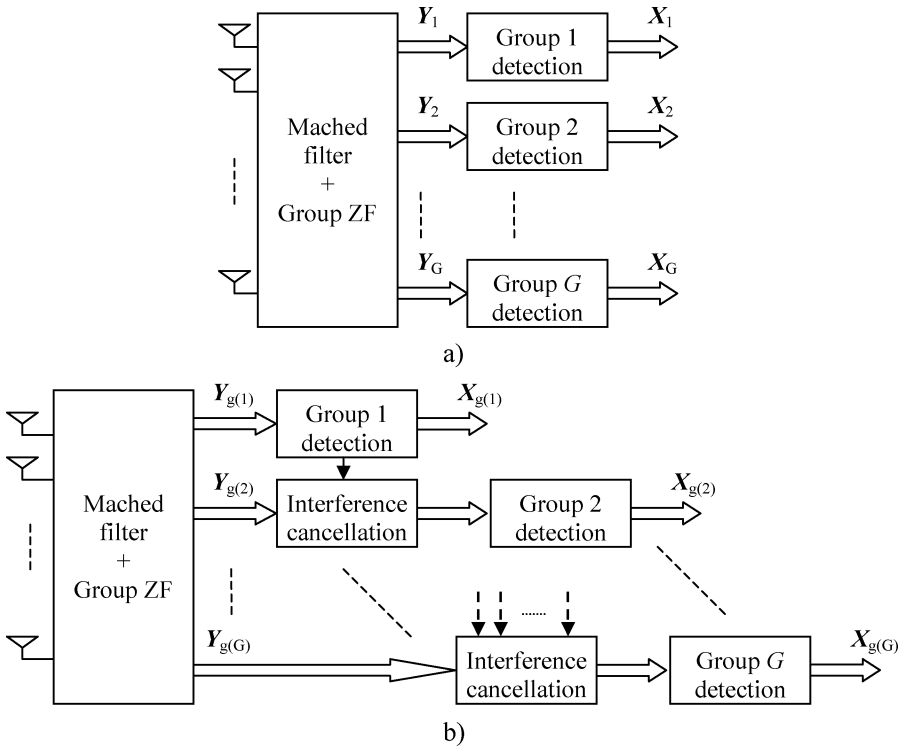

Fig. 2. a) GZF receiver block diagram. b) GSIC receiver block diagram.

GZF receiver as shown in Fig. 2(a), each group g is associated with a sufficient statistic vector $\boldsymbol{Y}_g^{\mathrm{GZF}}$, such that [12], [13]

$$\boldsymbol{Y}_g^{\mathrm{GZF}} = \sqrt{\frac{\mathrm{SNR}}{K}}\boldsymbol{X}_g + \boldsymbol{V}_g \tag{2}$$

where $\boldsymbol{V}_g$ is $\mathcal{N}(\boldsymbol{0}, \boldsymbol{Q}_g)$ distributed and $\boldsymbol{Q}_g = [\boldsymbol{H}^\dagger \boldsymbol{H}]^{-1}_{(g)}$ is the gth diagonal submatrix of $[\boldsymbol{H}^\dagger \boldsymbol{H}]^{-1}$, of size $|g|$ with $(\cdot)^\dagger$ denoting the complex conjugate transpose operator. When GSIC is considered, interference cancellation of the already detected groups is performed successively, as shown in Fig. 2(b). In contrast to the GZF architecture, the order in which the various groups are detected plays an important role with GSIC. Let $g(i)$ denote the group detected at the ith stage. A sufficient statistic vector at the ith stage is then given by

$$\boldsymbol{Y}_{g(i)}^{\mathrm{GSIC}} = \sqrt{\frac{\mathrm{SNR}}{K}}\boldsymbol{X}_{g(i)} + \Gamma_{g(i)} + \boldsymbol{V}_{g(i)} \tag{3}$$

where $\Gamma_{g(i)}$ is the residual interference due to decision errors. Let $\boldsymbol{H}(i)$ denote the equivalent channel after interference cancellation. $\boldsymbol{V}_{g(i)}$ is then $\mathcal{N}(\boldsymbol{0}, \boldsymbol{Q}_{g(i)})$ distributed with $\boldsymbol{Q}_{g(i)} = [\boldsymbol{H}(i)^\dagger \boldsymbol{H}(i)]^{-1}_{(g(i))}$.

Throughout this paper, we denote by $\det(\cdot)$ and $\mathrm{trace}(\cdot)$ the determinant and the trace operators, respectively. Finally, for an arbitrary matrix $\boldsymbol{A}$, we shall write $\boldsymbol{A} \geq 0$ when $\boldsymbol{A}$ is a Hermitian positive matrix.

III. Tradeoff Problem Formulation

Consider the channel $\boldsymbol{H}$ over the G blocks of length ℓ, and derive the diversity-multiplexing tradeoff performance functions with GZF and GSIC. In [2], the diversity-multiplexing tradeoff function of a given scheme is defined as the SNR exponent function of the minimum frame-error rate (FER) of that same scheme, achieved when the best outer codes that generate the transmitted symbols are used. Let $P_e(\mathrm{SNR})$ denote such minimum FER, and $d(r)$ its SNR exponent function, or the tradeoff function. r is defined as the system multiplexing rate, and is given by $r = R(\mathrm{SNR})/\log(\mathrm{SNR})$. Also, let $P_{\mathrm{out}}(R)$ denote the system outage probability, and $d_{\mathrm{out}}(r)$ its associated SNR exponent function. Throughout this paper, the following notation will be used:

$$f(\mathrm{SNR}) \doteq \mathrm{SNR}^b \text{ when } \lim_{\mathrm{SNR}\to\infty} \frac{\log f(\mathrm{SNR})}{\log \mathrm{SNR}} = b. \tag{4}$$

Accordingly, we can write

$$P_e(\mathrm{SNR}) \doteq \mathrm{SNR}^{-d(r)} \text{ and } P_{\mathrm{out}}(R) \doteq \mathrm{SNR}^{-d_{\mathrm{out}}(r)}. \tag{5}$$

It was found in [2] that $P_{\mathrm{out}}(R)$ is a lower bound of $P_e(\mathrm{SNR})$. Moreover, when $\ell \geq N + K - 1$, $P_{\mathrm{out}}(R)$ also upper bounds $P_e(\mathrm{SNR})$. The tradeoff function $d(r)$ is, hence, given by $d(r) = d_{\mathrm{out}}(r)$. Using a similar approach, we evaluate in what follows the overall outage probability for GZF and GSIC receivers, and deduce their corresponding tradeoff performance functions, that we denote by $d^{\mathrm{GZF}}(r)$ and $d^{\mathrm{GSIC}}(r)$, respectively.

A. Group Outage Probability

We derive in what follows an expression for the overall outage event according to the system configuration. Denote by H the random realization of the channel $\boldsymbol{H}$ over the considered time frame ℓ. Consider the system given in (1), and let $I_H = I(\boldsymbol{X}; \boldsymbol{Y} | \boldsymbol{H} = H)$ be its mutual information conditioned on $\boldsymbol{H} = H$ [7]. When the system in (1) does not meet its

required data rate R, an outage event takes place, which we denote by $\Omega_{\text{out},H}$ and we write as

$$\Omega_{\text{out},H} = \{H : I_H < R\}.$$

The overall system outage probability is then given by $P_{\text{out}}(R) = P(\Omega_{\text{out},H})$. When group detection is used, an overall outage event indicates that any of the considered groups is in outage.

Definition 1: Let $\Omega_{g_{\text{out},H}}$ denote the gth group outage event, associated with an input $\boldsymbol{X}_g$, an output $\boldsymbol{Y}_g$, a data rate R_g, and a random channel realization $\boldsymbol{H} = H$ held fixed for all the time. $\Omega_{g_{\text{out},H}}$ is defined as the event where the gth group does not meet its required data rate R_g, and is written as

$$\Omega_{g_{\text{out},H}} = \{H : I_{g,H} < R_g\}$$

where $I_{g,H} = I(\boldsymbol{X}_g; \boldsymbol{Y}_g | \boldsymbol{H} = H)$ is the gth-group mutual information. The group outage probability is then defined as the probability of $\Omega_{g_{\text{out},H}}$, and is written as $P_{g,\text{out}}(R_g)$.

According to *Definition 1*, we can write the following:

$$\Omega_{\text{out},H} = \{H : I_H < R\} = \left\{ H : \bigcup_{g=1}^{G} \{I_{g,H} < R_g\} \right\}.$$

B. GZF Tradeoff Function

Using the results of Section III-A, we provide a closed-form expression of the overall tradeoff function for the GZF receiver. To do so, we first evaluate the SNR exponent of the outage probability, and then derive $d^{\text{GZF}}(r)$ using a similar approach to the one in [2].

According to (2) and in the case of a GZF receiver, the G group outage events are independent of each other. This implies that

$$\begin{aligned}\Omega_{\text{out},H} &= \left\{ \bigcup_{g=1}^{G} \left\{ H : I_{g,H}^{\text{GZF}} < R_g \right\} \right\} \\ &= \Omega_{1_{\text{out},H}} \cup \Omega_{2_{\text{out},H}} \cup \ldots \cup \Omega_{G_{\text{out},H}}\end{aligned}$$

and

$$P(\Omega_{\text{out},H}) = 1 - \prod_{g=1}^{G} \left[1 - P\left(\Omega_{g_{\text{out},H}}\right) \right].$$

Consequently, the overall system outage probability with GZF satisfies

$$P_{\text{out}}^{\text{GZF}}(R) = 1 - \prod_{g=1}^{G} \left[1 - P_{g,\text{out}}^{\text{GZF}}(R_g) \right] \tag{6}$$

where $P_{g,\text{out}}^{\text{GZF}}(R_g)$ is as defined for the gth group with GZF according to *Definition 1*. Now, using the union bound, as well as the fact that the overall system outage probability is lower bounded by the worst group outage performance, (6) gives

$$\max_{g=1,\ldots,G} \left\{ P_{g,\text{out}}^{\text{GZF}}(R_g) \right\} \leq P_{\text{out}}^{\text{GZF}}(R) \leq \sum_{g=1}^{G} P_{g,\text{out}}^{\text{GZF}}(R_g). \tag{7}$$

Let $R_g(\text{SNR})$ be written as $R_g(\text{SNR}) = r_g \log(\text{SNR})$, with $r = \sum_{g=1}^{G} r_g$. Also, let $d_{g,\text{out}}^{\text{GZF}}(r_g)$ denote the SNR exponent of $P_{g,\text{out}}^{\text{GZF}}(R_g)$. According to (4), we can write

$$P_{g,\text{out}}^{\text{GZF}}(R_g) \doteq \text{SNR}^{-d_{g,\text{out}}^{\text{GZF}}(r_g)}. \tag{8}$$

At high SNR values, the union bound in (7) decays exponentially with the worst group performance. Hence

$$\begin{aligned}P_{\text{out}}^{\text{GZF}}(R) &\doteq \text{SNR}^{-d_{\text{out}}^{\text{GZF}}(r)} \text{ with } d_{\text{out}}^{\text{GZF}}(r) \\ &= \left\{ \min_{g=1,\ldots,G} \left\{ d_{g,\text{out}}^{\text{GZF}}(r_g) \right\}; \sum_{g=1}^{G} r_g = r \right\}. \end{aligned} \tag{9}$$

For a sufficiently long block length that we specify in the next section, $P_{\text{out}}^{\text{GZF}}(R)$ is both a lower and an upper bound of $P_e^{\text{GZF}}(\text{SNR})$. Consequently, $P_e^{\text{GZF}}(\text{SNR}) \doteq P_{\text{out}}^{\text{GZF}}(R)$. Since $P_e^{\text{GZF}}(\text{SNR}) \doteq \text{SNR}^{-d^{\text{GZF}}(r)}$, then using (9), the overall GZF tradeoff function satisfies

$$\begin{aligned}d^{\text{GZF}}(r) &= d_{\text{out}}^{\text{GZF}}(r) = d_{g_{\text{worst}}}^{\text{GZF}}(r) \\ &= \left\{ \min_{g=1,\ldots,G} \left\{ d_{g,\text{out}}^{\text{GZF}}(r_g) \right\}; \sum_{g=1}^{G} r_g = r \right\} \end{aligned} \tag{10}$$

where g_{worst} denotes the group with the worst tradeoff performance.

C. GSIC Tradeoff Function

When the GSIC architecture is used, the group outage events $\{\Omega_{g_{\text{out},H}}\}$ are no longer independent. In order to evaluate the GSIC tradeoff function, we resort to the use of the genie approach [6], [14]. The latter feeds back the correct data estimation to the GSIC receiver, so as to eliminate the residual interference term $\Gamma_{g(i)}$ in (3). By doing so, (3) is rewritten as

$$\boldsymbol{Y}_{g(i)}^{\text{genie}} = \sqrt{\frac{\text{SNR}}{K}} \boldsymbol{X}_{g(i)} + \boldsymbol{V}_{g(i)}.$$

Since the genie receiver provides the same overall FER performance as the original GSIC receiver [6], [14], we conclude that these two receivers have the same minimum achievable FER with the best outer codes, as well as the same tradeoff functions. Hence, $P_e^{\text{GSIC}}(\text{SNR}) = P_e^{\text{genie}}(\text{SNR})$ and $d^{\text{GSIC}}(r) = d^{\text{genie}}(r)$. The problem consists now in evaluating $d^{\text{genie}}(r)$. Consider the group outage events obtained with the genie receiver. These quantities are clearly independent of each other [6], [14]. $d^{\text{genie}}(r)$ could then be obtained following a similar approach to the one in Section III-B. However, we propose in what follows another method to obtain the same result. Specifically, we evaluate the SNR exponent of each group FER or each group tradeoff function, and then deduce the overall system performance.

Let $P_{g(i),\text{out}}^{\text{genie}}(R_{g(i)})$ be the outage probability of the $g(i)$th group. Also, let $P_{e,g(i)}^{\text{genie}}(\text{SNR})$ denote its minimum FER and $d_{g(i)}^{\text{genie}}(r_{g(i)})$ its corresponding SNR exponent function. It can be easily shown that for each group $g(i)$ and for a sufficiently long

block length, we have $d^{\text{genie}}_{g(i)}(r_{g(i)}) = d^{\text{genie}}_{g(i),\text{out}}(r_{g(i)})$. Then, similar to (8), the overall FER is bounded as [12], [13]

$$\max_{i=1,\ldots,G}\left\{P^{\text{genie}}_{e,g(i)}(\text{SNR})\right\} \le P^{\text{genie}}_{e}(\text{SNR}) \le \sum_{i=1}^{G} P^{\text{genie}}_{e,g(i)}(\text{SNR}). \tag{11}$$

At high SNR values g_{worst}, the group with the worst performance dominates both bounds. As a consequence

$$\begin{aligned} d^{\text{GSIC}}(r) &= d^{\text{genie}}(r) = d^{\text{genie}}_{g_{\text{worst}}}(r) \\ &= \left\{ \min_{i=1,\ldots,G}\left\{ d^{\text{genie}}_{g(i)}\left(r_{g(i)}\right)\right\}; \sum_{i=1}^{G} r_{g(i)} = r \right\}. \end{aligned} \tag{12}$$

IV. Group Outage Probability and Tradeoff

In this section, we explicitly evaluate the tradeoff functions of GZF and GSIC. According to (10) and (12), these functions, $d^{\text{GZF}}(r)$ and $d^{\text{GSIC}}(r)$, respectively, depend on the tradeoff functions of all the groups. Using the channel statistics properties, we evaluate here the performance of each of the groups. We first consider the case of GZF and generalize the obtained results to the case with GSIC.

Consider the gth group, and denote by $\mathcal{H}(.)$ the entropy function and $\boldsymbol{\mathcal{E}}(.)$ the expectation operator. According to (2) and *Definition 1*, we have

$$\begin{aligned} \boldsymbol{I}(\boldsymbol{X}_g;\boldsymbol{Y}_g|\boldsymbol{H}=H) &= \mathcal{H}(\boldsymbol{Y}_g|\boldsymbol{H}=H) - \mathcal{H}(\boldsymbol{Y}_g|\boldsymbol{X}_g;\boldsymbol{H}=H) \\ &= \log\det\left(\boldsymbol{Q}_g + \frac{\text{SNR}}{K}\boldsymbol{\mathcal{E}}\left(\boldsymbol{X}_g\boldsymbol{X}_g^{\dagger}\right)\right) \\ &\quad - \log\det(\boldsymbol{Q}_g). \end{aligned} \tag{13}$$

A similar approach to the one in [2] allows us to choose the transmitted data to be Gaussian distributed with a covariance matrix $K\boldsymbol{I}_{|g|}$. (13) is then simplified to

$$I(\boldsymbol{X}_g;\boldsymbol{Y}_g|\boldsymbol{H}=H) = \log\frac{\det\left(\boldsymbol{Q}_g + \text{SNR}\times\boldsymbol{I}_{|g|}\right)}{\det(\boldsymbol{Q}_g)}. \tag{14}$$

According to Section II, $\boldsymbol{H}^{\dagger}\boldsymbol{H} \ge 0$ and of full rank K. It follows that $\boldsymbol{Q}_g \ge 0$ and is also of full rank $|g|$. Let $\alpha_1 \le \alpha_2 \le \cdots \le \alpha_{|g|}$ be the ordered eigenvalues of $\boldsymbol{Q}_g$. Accordingly, (14) is rewritten as

$$I(\boldsymbol{X}_g;\boldsymbol{Y}_g|\boldsymbol{H}=H) = \log\prod_{i=1}^{|g|}\left(1+\text{SNR}\frac{1}{\alpha_i}\right). \tag{15}$$

Consider the inverse of $\boldsymbol{Q}_g$, $\boldsymbol{Q}_g^{-1}$. The latter is ≥ 0 and of full rank $|g|$. Let $\{\mu_1,\mu_2,\ldots,\mu_{|g|}\}$ denote its ordered eigenvalues, such that $\mu_i = 1/\alpha_{|g|-i+1}$, $\forall i = 1,\ldots,|g|$. Using (15) and *Definition 1*, the gth group outage probability satisfies

$$P^{\text{GZF}}_{g,\text{out}}(R_g) \doteq P\left[\log\prod_{i=1}^{|g|}(1+\text{SNR}\mu_i) < R_g\right]. \tag{16}$$

In Appendix A, we show that $\{\mu_1,\mu_2,\ldots,\mu_{|g|}\}$ have the following joint probability density function (pdf):

$$\begin{aligned} p\left(\mu_1,\mu_2,\ldots,\mu_{|g|}\right) &= C^{-1}_{|g|,N-|\overline{g}|} e^{-\sum_{i=1}^{|g|}\mu_i} \\ &\quad \times \prod_{i=1}^{|g|}\mu_i^{|N-|\overline{g}|-|g||}\prod_{j<i}(\mu_j-\mu_i)^2 \end{aligned} \tag{17}$$

where $|\overline{g}|$ denotes the number of interferers with the gth group. Since we assume a GZF receiver, $|\overline{g}|$ will be written as $|\overline{g}|^{\text{GZF}}$, and is given by $|\overline{g}|^{\text{GZF}} = K - |g|$.

According to (17), $d^{\text{GZF}}_{g,\text{out}}(r_g)$ can be obtained with a similar approach to the one in [2]. Thus, $d^{\text{GZF}}_{g,\text{out}}(r_g)$ is found to connect the points $(k, d^{\text{GZF}}_{g,\text{out}}(k))$, such that

$$d^{\text{GZF}}_{g,\text{out}}(k) = \left(N - |\overline{g}|^{\text{GZF}} - k\right)\left(|g|-k\right),\ k\in\{1,\ldots,|g|\}. \tag{18}$$

Let $\ell^{\text{GZF}}_{\min} = N-K+2|g_{\text{worst}}|-1$. Given (10) and (18) and using the results in [2], we can conclude that $d^{\text{GZF}}(r) = d^{\text{GZF}}_{\text{out}}(r)$ when $\ell \ge \ell^{\text{GZF}}_{\min}$.

In the case of the GSIC receiver, $\{\mu_1,\mu_2,\ldots,\mu_{|g(i)|}\}$ have the same distribution as in (17), but with

$$|\overline{g(i)}| = |\overline{g(i)}|^{\text{GSIC}} = \sum_{j=g+1}^{G}|g(j)|.$$

Hence, $d^{\text{genie}}_{g(i),\text{out}}(r_{g(i)})$ connects the points $(k, d^{\text{genie}}_{g(i),\text{out}}(k))$ such that

$$\begin{aligned} d^{\text{genie}}_{g(i),\text{out}}(k) &= \left(N - \left|\overline{g(i)}\right|^{\text{GSIC}} - k\right)\left(|g(i)|-k\right), \\ &\qquad k\in\{1,\ldots,|g(i)|\}. \end{aligned} \tag{19}$$

The tradeoff function $d^{\text{GSIC}}(r)$ is thus given by (12) when $\ell \ge \ell^{\text{GSIC}}_{\min}$, with $\ell^{\text{GSIC}}_{\min} = N - |\overline{g}_{\text{worst}}|^{\text{GSIC}} + |g_{\text{worst}}| - 1$.

V. Rate Allocation

The rate allocated to each of the groups plays obviously an important role in the evaluation of the system-tradeoff performance. We consider in what follows three rate allocations; namely, equal-rate allocation, group-size proportional rate allocation, and optimal-rate allocation. $d^{\text{GZF}}(r)$ and $d^{\text{GSIC}}(r)$ are then evaluated accordingly. Table I summarizes the various notations used for the tradeoff functions in all of these cases. Furthermore, (18) and (19) indicate that different partitions will lead to different tradeoff performances. Consequently, we optimize $d^{\text{GZF}}(r)$ and $d^{\text{GSIC}}(r)$ with regard to the group partitioning. Two steps of optimization are considered here. First, the number of groups G is held fixed. We denote the tradeoff in this case by the optimized tradeoff. Second, G is varied to obtain an overall optimum tradeoff function.

In the remainder of this section, we assume a sufficiently long block length ℓ, as mentioned in Section IV. We consider a random partition $\{p, G\}$, and denote by g_1 the group with the

TABLE I
OVERALL TRADEOFF NOTATIONS. EXAMPLE: GZF

	Equal rate allocation	***Size proportional allocation***	***Optimal allocation***
Tradeoff with a random partition $\{p,G\}$	$d^{GZF,\{p,G\}}_{EqRate}(r)$	$d^{GZF,\{p,G\}}_{PropRate}(r)$	$d^{GZF,\{p,G\}}_{OptRate}(r)$
Optimized tradeoff	$d^{GZF}_{EqRate}(G,r)$	$d^{GZF}_{PropRate}(G,r)$	$d^{GZF}_{OptRate}(G,r)$

largest size, by g_2 the one with the second-largest size, and so on. We have, then, $|g_1| \geq |g_2| \geq \ldots \geq |g_G|$.

A. Equal-Rate Allocation

Consider the GZF receiver. Assuming equal-rate allocation, we have $r_{g_i} = r/G$. (10) and (18) allow us to write, in this case

$$d^{\mathrm{GZF},\{p,G\}}_{\mathrm{EqRate}}(r) = \min_{i=1,\ldots,G}\left\{d^{\mathrm{GZF}}_{g_i}(r)\right\} = d^{\mathrm{GZF}}_{g_G}\left(\frac{r}{G}\right) = \left(N-K+|g_G|-\frac{r}{G}\right)\left(|g_G|-\frac{r}{G}\right) \quad (20)$$

with $r \in [0, G\times|g_G|]$. Clearly, the maximum achievable multiplexing rate with this allocation is $G\times|g_G|$, which is smaller than K.

For the optimization of $d^{\mathrm{GZF},\{p,G\}}_{\mathrm{EqRate}}(r)$ over all possible partitions with G groups, we can conclude, using (20), that $d^{\mathrm{GZF},\{p,G\}}_{\mathrm{EqRate}}(r)$ is maximized when the smallest group size $|g_G|$ is maximized. That is, when $\{p,G\}$ approaches the equal-size partition and $|g_G| = \lfloor K/G \rfloor$. Let $d^{\mathrm{GZF}}_{\mathrm{EqRate}}(G,r)$ denote the optimized tradeoff in this case. Then

$$d^{\mathrm{GZF}}_{\mathrm{EqRate}}(G,r) = \left(N-K+\left\lfloor\frac{K}{G}\right\rfloor-\frac{r}{G}\right)\left(\left\lfloor\frac{K}{G}\right\rfloor-\frac{r}{G}\right). \quad (21)$$

Now, by varying G in a second step, (21) indicates that $d^{\mathrm{GZF}}_{\mathrm{EqRate}}(G,r)$ is further maximized when $G=2$. The overall optimum tradeoff performance is thus obtained.

When GSIC is used, the group-detection order plays an important role in evaluating the overall tradeoff performance $d^{\mathrm{GSIC},\{p,G\}}_{\mathrm{EqRate}}(r)$. In Appendix B-A, we show that $d^{\mathrm{GSIC},\{p,G\}}_{\mathrm{EqRate}}(r)$ is maximized when the groups are retrieved in the decreasing order of their sizes. (12) and (19) are, hence, rewritten as

$$d^{\mathrm{GSIC}}_{g_i}(r) = \left(N-|\overline{g_i}|^{\mathrm{GSIC}}-\frac{r}{G}\right)\left(|g_i|-\frac{r}{G}\right)$$
$$d^{\mathrm{GSIC}\{p,G\}}_{\mathrm{EqRate}}(r) = \min_{i=1,\ldots,G}\left\{d^{\mathrm{GSIC}}_{g_i}(r)\right\} \quad (22)$$

The exact evaluation of $d^{\mathrm{GSIC},\{p,G\}}_{\mathrm{EqRate}}(r)$ turns out to be analytically difficult, and we will use computer simulations to do it. However, when all the groups have the same size L, the problem is simplified, and the tradeoff function is given by $(N-(G-1)L-(r/G))(L-(r/G))$. The GSIC and GZF have equivalent performances in this case. Finally, both optimization steps of $d^{\mathrm{GSIC},\{p,G\}}_{\mathrm{EqRate}}(r)$ will be applied using computer simulations.

B. Size-Proportional Rate Allocation

With this algorithm, groups are allocated rates proportionally to their size. Hence, $r_{g_i} = r|g_i|/K$ with $r \in [0,K]$. Note here that the maximum achievable multiplexing rate is K, in contrast to the equal rate-allocation algorithm.

Using (10) and (18), the overall GZF tradeoff function is simplified to

$$d^{\mathrm{GZF},\{p,G\}}_{\mathrm{PropRate}}(r) = |g_G|\left(N-K+|g_G|-\frac{r}{K}|g_G|\right)\left(1-\frac{r}{K}\right). \quad (23)$$

The optimized tradeoff function for a given G, $d^{\mathrm{GZF}}_{\mathrm{PropRate}}(G,r)$, is also achieved when $|g_G| = \lfloor K/G \rfloor$, and the overall optimum performance is obtained with $G=2$.

As for the GSIC receiver, it can be shown that the tradeoff function obtained with $\{p,G\}$ is maximized when the groups are retrieved in the decreasing order of their sizes. As a result

$$d^{\mathrm{GSIC}}_{g_i}(r) = |g_i|\left(N-|\overline{g_i}|^{\mathrm{GSIC}}-\frac{r}{K}|g_i|\right)\left(1-\frac{r}{K}\right)$$
$$d^{\mathrm{GSIC},\{p,G\}}_{\mathrm{PropRate}}(r) = \min_{i=1,\ldots,G}\left\{d^{\mathrm{GSIC}}_{g_i}(r)\right\}. \quad (24)$$

Exact evaluation of $d^{\mathrm{GSIC},\{p,G\}}_{\mathrm{PropRate}}(r)$ and its optimized functions will all be obtained using computer simulations. Finally, when all the groups have the same size, we can easily verify that the size-proportional rate allocation achieves the same performance as the equal-rate one with both receivers.

C. Optimal-Rate Allocation With GZF

The optimal rate-allocation algorithm aims to

$$\text{maximize } d^{\mathrm{GZF}}(r) = \min_{g=1,\ldots,G}\left\{d^{\mathrm{GZF}}_{g}(r_g)\right\}$$
$$\text{subject to: } \left\{\sum_{g=1}^{G} r_g = r; r_g \in [0,|g|], \forall g = 1,\ldots,G\right\}. \quad (25)$$

Let $d^{\mathrm{GZF},\{p,G\}}_{\mathrm{OptRate}}(r)$ denote the obtained tradeoff function for the partition $\{p,G\}$. Allocation in this case is performed in G slots of multiplexing rates, where only "j" groups are allocated rates that are not zero at the jth slot. Let $\{[r^{(0)},r^{(1)}],[r^{(1)},r^{(2)}],\ldots,[r^{(G-1)},r^{(G)}]\}$ denote these slots, where $\{r^{(0)},r^{(1)},\ldots,r^{(G)}\}$ will be evaluated later in this section. Also, let the diversity gain corresponding to $r^{(j)}$ be written as $d^{\mathrm{GZF},\{p,G\}}_{\mathrm{OptRate}}(j)$. The overall tradeoff function will then connect the points $(r^{(j)}, d^{\mathrm{GZF},\{p,G\}}_{\mathrm{OptRate}}(j))$ for $j=0,\ldots,G$.

Since the optimal-rate allocation maximizes the overall tradeoff performance, then both $r^{(j)}$ and $d^{\mathrm{GZF},\{p,G\}}_{\mathrm{OptRate}}(j)$ should be maximized for each j. Consequently, $r^{(j)}$ is the maximum starting rate from which $(j+1)$ groups are active, and $d^{\mathrm{GZF},\{p,G\}}_{\mathrm{OptRate}}(j)$ is the best possible diversity achieved with $(j+1)$ active groups, out of G groups. $d^{\mathrm{GZF},\{p,G\}}_{\mathrm{OptRate}}(r)$ is next fully specified as follows.

- Let $r^{(0)}=0$, $r^{(G)}=K$, and $d_{\text{OptRate}}^{\text{GZF},\{p,G\}}(G)=0$. $d_{\text{OptRate}}^{\text{GZF},\{p,G\}}(r)$ connects the points $(r^{(j)}, d_{\text{OptRate}}^{\text{GZF},\{p,G\}}(j))$, $j=0,\ldots,G$, such that

$$d_{\text{OptRate}}^{\text{GZF},\{p,G\}}(j)=\left(N-K^{(j)}\right)|g_{j+1}|, \quad \text{for } j=0,\ldots,G-1 \tag{26}$$

$$r^{(j)}=\frac{Nj}{2}+\left(1-\frac{j}{2}\right)K^{(j)}-\frac{j}{2}\sqrt{\Delta^{(j)}}, \quad \text{for } j=1,\ldots,G-1 \tag{27}$$

with $K^{(j)}=\sum_{k=1}^{j}|g_k|$, $A^{(j)}=N-K^{(j)}$, and $\Delta^{(j)}=(A^{(j)})^2+4A^{(j)}|g_{j+1}|$.

- When $r\in[r^{(j-1)},r^{(j)}]$, only $\{g_1,g_2,\ldots,g_j\}$ are allocated a nonzero rate $r_{g_i}(j)$, such that

$$r_{g_i}(j)=\frac{1}{j}\left(r+j|g_i|-K^{(j)}\right). \tag{28}$$

The corresponding diversity gain to the considered multiplexing rate r is given by

$$d_{\text{OptRate}}^{\text{GZF},\{p,G\}}(r)=\left(N-\frac{r}{j}\right)\left(K^{(j)}-\frac{r}{j}\right), \quad \text{for } j=1,\ldots,G. \tag{29}$$

The diversity-gain expression provided in (26) is the maximum achievable gain, with $(j+1)$ active groups out of G groups. It is obtained according to (18) when the corresponding multiplexing rate of all the $(j+1)$ selected groups are equal to zero. In Appendix B-B, we show that $d_{\text{OptRate}}^{\text{GZF},\{p,G\}}(j)$ is maximized when these $(j+1)$ selected groups are the ones with the largest sizes, i.e., $\{g_1,g_2,\ldots,g_{j+1}\}$. (26) follows then immediately. As for $\{r^{(1)},r^{(2)},\ldots,r^{(G-1)}\}$, they are derived in Appendix B-C using (26). We can easily verify that $r^{(j)}$ given in (27) is indeed the best possible starting rate from which $(j+1)$ groups are active. In fact, we have $(\partial r^{(j)}/\partial K^{(j)})\geq 0$ for any $j\in\{1,\ldots,G\}$. This implies that $\forall j\in\{1,\ldots,G\}$, $r^{(j)}$ is maximized when the total number of active antennas for the jth slot is maximized. That is, when $\{g_1,g_2,\ldots,g_j\}$ are the only groups allocated rates different than zero, and when $\{g_1,g_2,\ldots,g_{j+1}\}$ are the next ones.

When $r\in[r^{(j-1)},r^{(j)}]$, (28) is derived in Appendix B-D using the following conditions:

$$\begin{cases}\sum_{i=1}^{j} r_{g_i}(j)=r\\ d_{g_i}^{\text{GZF},\{p,G\}}\left(r_{g_i}(j)\right)=d_{g_1}^{\text{GZF},\{p,G\}}\left(r_{g_1}(j)\right)\\ \quad \forall i=1,2,\ldots,j.\end{cases} \tag{30}$$

The overall diversity gain, given in (29), is then obtained using (18) and (28). It can be easily verified here that this diversity gain is maximized when $\{g_1,g_2,\ldots,g_j\}$ are the only active groups at the jth slot. The result provided in (29) indicates that when $r\in[r^{(j-1)},r^{(j)}]$, GZF is equivalent to the optimal detection applied to a MIMO system with N receive antennas, $K^{(j)}$ transmit antennas, and equal-rate allocation.

We further optimize $d_{\text{OptRate}}^{\text{GZF},\{p,G\}}(r)$ over all possible partitions with G groups to obtain $d_{\text{OptRate}}^{\text{GZF}}(G,r)$. According to the provided algorithm in (26)–(29), $d_{\text{OptRate}}^{\text{GZF},\{p,G\}}(r)$ and $\{r^{(0)},r^{(1)},\ldots,r^{(G-1)}\}$ are maximized when $K^{(j)}$ is maximized for any $j\in\{1,\ldots,G\}$. Hence, $d_{\text{OptRate}}^{\text{GZF}}(G,r)$ is achieved with the partition $\{p^*,G\}=\{g_1^*,g_2^*,\ldots,g_G^*\}$ that maximizes $K^{(j)}$ for each j. That is

$$\begin{cases}|g_1^*|=K-G+1\\ |g_2^*|=\cdots=|g_G^*|=1.\end{cases} \tag{31}$$

$d_{\text{OptRate}}^{\text{GZF}}(G,r)$ is then given according to (26)–(29) with $\{p^*,G\}$ as a partition.

Finally, we further optimize $d_{\text{OptRate}}^{\text{GZF}}(G,r)$ with regard to the number of groups G. Results in (26)–(29) indicate that $d_{\text{OptRate}}^{\text{GZF}}(G,r)$ is maximized when G is decreased. Assuming the existence of at least two groups in the system, the overall optimum GZF tradeoff function is obtained with $\{p^*,2\}$. Numerical results will further confirm such a conclusion.

D. Optimal-Rate Allocation With GSIC

As in the case of GZF, the tradeoff function with optimal-rate allocation for the GSIC receiver connects the points $(r^{(j)}, d_{\text{OptRate}}^{\text{GSIC},\{p,G\}}(j))$ for $j=0,\ldots,G$. In this case, not only the groups being active for each rate r are important to allow the evaluation of the system-tradeoff performance, but also their detection order. At each multiplexing rate r, a different set of groups with different detection order might be deployed so as to maximize the tradeoff function. Let $g(i)$ denote the ith-detected group, being randomly chosen for a given value of r. Then, when $r\in[r^{(j-1)},r^{(j)}]$, (19) is rewritten as

$$d_{g(i)}^{\text{GSIC}}\left(r_{g(i)}\right)=\left(N-\left|\overline{g(i)}\right|^{\text{GSIC}}-r_{g(i)}\right)\left(|g_{g(i)}|-r_{g(i)}\right) \quad \forall i=1,\ldots,j. \tag{32}$$

Accordingly, we have $(\partial(d_{g(i)}^{\text{GSIC}}(r_{g(i)}))/\partial|g(i)|)\geq 0$. This implies that $d_{g(i)}^{\text{GSIC}}(r_{g(i)})$ is maximized only when $|g(i)|$ is maximized, and that $\min_{i=1,\ldots,j}\{d_{g(i)}^{\text{GSIC}}(r_{g(i)})\}$ is maximized only when $g(i)=g_i$ for any $i=1,\ldots,j$. In addition, we have $(\partial(d_{g(i)}^{\text{GSIC}}(r_{g(i)}))/\partial|\overline{g}(i)|^{\text{GSIC}})\leq 0$. It follows that $\min_{i=1,\ldots,j}\{d_{g(i)}^{\text{GSIC}}(r_{g(i)})\}$ is further maximized when $\{g_1,g_2,\ldots,g_j\}$ are retrieved in the decreasing order of their sizes. $d_{\text{OptRate}}^{\text{GSIC},\{p,G\}}(r)$ is obtained. A similar analysis for $r^{(j)}$ and $d_{\text{OptRate}}^{\text{GSIC},\{p,G\}}(j)$ provides the same conclusions. As a result, the tradeoff function with optimal-rate allocation for GSIC shall connect the points $(r^{(j)}, d_{\text{OptRate}}^{\text{GSIC},\{p,G\}}(j))$ $\forall j=0,\ldots,G$, such that

$$d_{\text{OptRate}}^{\text{GSIC},\{p,G\}}(j)=\min_{i=1,\ldots,j+1}\left\{d_{g_i}^{\text{GSIC}}\left(r_{g_i}=0\right)\right\} \tag{33}$$

and where $\{r^{(1)},r^{(2)},\ldots,r^{(G-1)}\}$ are obtained following a similar approach as the one in Appendix B-C for GZF. Moreover, when $r\in[r^{(j-1)},r^{(j)}]$, only $\{g_1,g_2,\ldots,g_j\}$ are allocated a nonzero rate $r_{g_i}(j)$, such that

$$\begin{cases}\sum_{i=1}^{j} r_{g_i}(j)=r\\ d_{g_i}^{\text{GSIC},\{p,G\}}\left(r_{g_i}(j)\right)=d_{g_1}^{\text{GSIC},\{p,G\}}\left(r_{g_1}(j)\right)\\ \quad \forall i=1,\ldots,j.\end{cases} \tag{34}$$

Since solving (33) and (34) turns out to be analytically difficult, we resort to computer simulations to evaluate $d_{\text{OptRate}}^{\text{GSIC},\{p,G\}}(r)$, as well as its optimized functions, according to the group partitions and the number of groups.

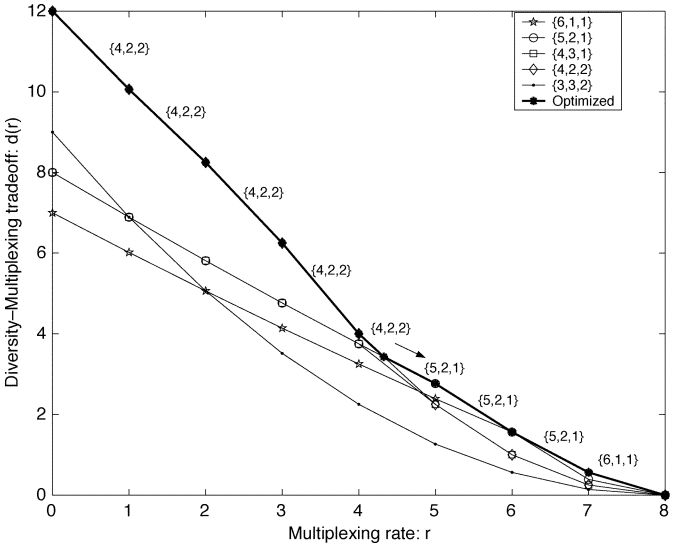

Fig. 3. Optimization of the GSIC tradeoff with size-proportional rate allocation. $N = K = 8$ and $G = 3$.

Finally, when all the groups have the same size L, the tradeoff function is simplified to a function that connects the points $(r^{(j)}, d_{\text{OptRate}}^{\text{GSIC},\{p,G\}}(j))$, such that

$$d_{\text{OptRate}}^{\text{GSIC},\{p,G\}}(j) = (N - jL)L \quad \forall j = 0, \ldots, G \tag{35}$$

$$r^{(0)} = 0$$

$$r^{(j)} = \frac{1}{2}\sum_{g=1}^{j}\left[A^{(j)} + (g+1)L - \sqrt{\Delta^{(j)}(g)}\right] \quad \forall j = 1, \ldots, G \tag{36}$$

with $\Delta^{(j)}(g) = [A^{(j)}]^2 + 2(g+1)A^{(j)}L + (g-1)^2L^2$, and $A^{(j)} = N - jL$.

VI. Simulation Results

In this section, we evaluate the diversity-multiplexing tradeoff of GZF, as well as GSIC with the three proposed rate-allocation algorithms. As described in Section V, we first evaluate the tradeoff with these allocations for a given partition $\{p, G\}$. We then optimize the obtained tradeoff results in two steps. The first step will be over all possible partitions for a given number of groups G. The second step will be over all possible partitions and numbers of groups. We assume throughout this section that $K = N = 8$ and $G \in \{2, 3, \ldots, K\}$. We shall denote by $\{|g_1|, |g_2|, \ldots, |g_G|\}$ an ordered group partition $\{p, G\}$, where $|g_i|$ refers to the size of its ith-detected group. Finally, we assume that the coding block length $\ell \geq \ell_{\min}^{\text{GZF}}$ or $\ell_{\min}^{\text{GSIC}}$.

A. Equal-Rate and Size-Proportional Rate Allocation

We will compare in this section the performance of the equal and the size-proportional allocation algorithms obtained with a random partition, as well as after optimization with regards to the group partition. We begin by considering the case of GSIC and illustrate how its optimized tradeoff is obtained. Also, assume the size-proportional allocation with $G = 3$. In Fig. 3, we plot the performance of all possible partitions, as indicated in Table II. $d_{\text{PropRate}}^{\text{GSIC}}(3, r)$ is obtained by selecting, *for each value of* r, the best possible achieved tradeoff performance. Fig. 3 indicates the selected partition for each r to illustrate this optimization process. For example, we observe that the {4,2,2} partition optimizes the tradeoff when $r \in [0, 4.3]$, followed by {5,2,1} and {6,1,1}. Clearly, different partitions are selected for different values of r. This is because the overall GSIC tradeoff function is not monotonously varying with regards to the group sizes, as shown in Fig. 3.

TABLE II
Group Partitioning, $K = 8$

G	*Possible partitions*
2	{7,1}; {6,2}; {5,3}; {4,4}
3	{6,1,1}; {5,2,1}; {4,3,1}; {4,2,2}; {3,3,2}
4	{5,1,1,1}; {4,2,1,1}; {3,3,1,1}; {3,2,2,1}; {2,2,2,2}
5	{4,1,1,1,1}; {3,2,1,1,1}; {2,2,2,1,1}
6	{3,1,1,1,1,1}; {2,2,1,1,1,1}
7	{2,1,1,1,1,1,1}
8	{1,1,1,1,1,1,1,1}

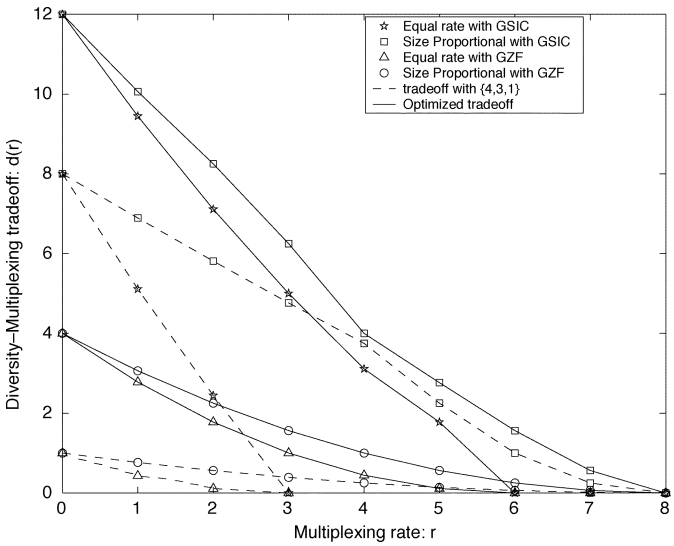

Fig. 4. Equal rate and size-proportional rate allocation performance with GZF and GSIC. $N = K = 8$ and $G = 3$.

A similar process can be applied to the GZF receiver to obtain $d_{\text{PropRate}}^{\text{GZF}}(3, r)$. The obtained numerical results which we do not include in Fig. 3 indicate that $d_{\text{PropRate}}^{\text{GZF}}(3, r)$ can be obtained with the {4,2,2} partition or the {3,3,2} one. These partitions indeed satisfy $|g_G| = \lfloor K/G \rfloor = 2$ and confirm conclusions derived in Section V-B. We shall note here that the optimized performance of GSIC is not only achieved with different partitions for different values of r, such as is the case with GZF, but also these partitions do not necessarily satisfy the condition $|g_G| = \lfloor K/G \rfloor$.

In Fig. 4, we assess the performance of the {4,3,1} partition, as well as the optimized one, when $G = 3$. First, consider the case of the {4,3,1} partition. Results indicate that the size-proportional scheme outperforms the equal-rate one for both receivers. A maximum rate $r_{\max} = 8$ sym/s (that is, $\min(N, K)$ sym/s) is achieved with this allocation, versus only 3 sym/s with the equal-rate one. As for the diversity gains, although both allocations achieve the same maximum diversity, the size-proportional scheme provides a diversity gain on the order of one for

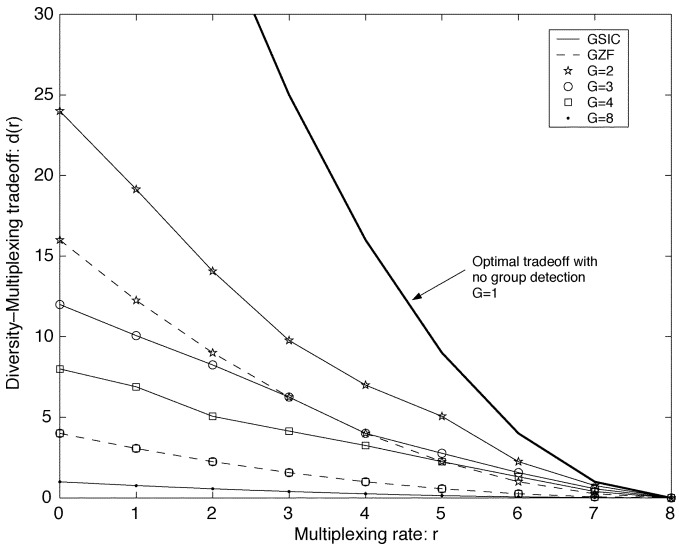

Fig. 5. Effect of G on the optimized tradeoff with size-proportional rate for GSIC and GZF. $N = K = 8$.

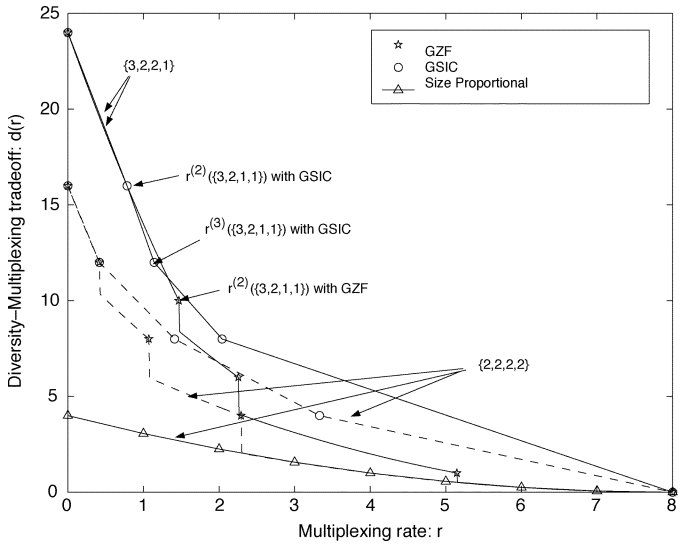

Fig. 6. Tradeoff performance of GSIC and GZF with optimum-rate allocation. $N = K = 8$ and $G = 4$.

any $r > 0$. Finally, GSIC is also observed to outperform GZF with both allocations.

Next, we compare in Fig. 4 the performance of the {4,3,1} partition with the optimized one. Significant tradeoff gains are demonstrated with the optimized performance. For example, an enhancement by 3 sym/s in the maximum multiplexing rate with the equal-rate allocation for both receivers is observed, as well as significant diversity gains. However, in the case of the size-proportional allocation with GSIC, comparison results of the optimized performance with the {4,3,1} partition indicate that only a little performance enhancement is obtained when $r > 4$ sym/s. Further, we observe in the case of GSIC that the optimized tradeoff with equal-rate allocation approaches the one with size proportional for all values of r. Hence, with GSIC, equal-rate allocation can be used, instead of the size-proportional one, to provide similar levels of optimized performance with lower complexity levels.

In Fig. 5, we investigate the effect of the number of groups G on the optimized tradeoff with the proportional-rate allocation. To do so, we consider the cases of $G = 2$, 3, 4, and 8. Results indicate that with GSIC, the tradeoff is *strictly* maximized when G is minimized. $G = 2$ indeed presents the best tradeoff among all possible values of G, approaching the optimal performance [2] for all values of r. When $G = 8$, all groups have the same size, 1. The GSIC receiver in this case is then equivalent to BLAST [6], and our obtained tradeoff confirms the one found in [2]. Hence, when group detection is used with $G < K$, GSIC strictly outperforms BLAST, and approaches the optimal performance [2] with much less complexity, thus demonstrating a major advantage of group detection.

As for the GZF receiver, diversity degradations are observed with $G = 2$, 3, and 4, compared with GSIC. Fig. 5 also indicates that the same optimized tradeoff is obtained with $G = 3, 4$ with GZF. This is explained by the fact that both partitions have the same $|g_G|$ as well as $|\overline{g_G}|^{\mathrm{GZF}}$. We note here that the same conclusion is not expected with the equal rate-allocation scheme. Finally, when $G = 8$, GSIC and GZF have equivalent performances. This further confirms the results obtained in Section V-B.

B. Optimal-Rate Allocation

We consider the performance of GZF and GSIC with optimal-rate allocation. To do so, we first assume that $G = 4$ and consider the partitions {3,2,2,1} and {2,2,2,2}. Fig. 6 presents the obtained tradeoffs, as well as the performance with the size-proportional scheme with {2,2,2,2} for comparison. When GZF is deployed, the tradeoff curve with the optimal-allocation scheme is obtained by evaluating the diversity for each r, according to the results in Section V-C. As for GSIC, we compute $(r^{(j)}, d_{\mathrm{OptRate}}^{\mathrm{GSIC},\{p,G\}}(j))$ for $j = 0, \ldots, G$, according to Section V-D, and approximate the tradeoff by a linear function connecting these points. To confirm the optimality of these points, we have evaluated for each point the tradeoff of each possible permutation of j out of G groups, and found that the results confirm our claims made in Section V-D.

A close observation of Fig. 6 indicates that the optimum-rate allocation significantly outperforms the size-proportional one for low values of r. However, when $r > 5$ sym/s, both schemes perform similarly to GZF. As for the comparison of GSIC with GZF, we first note that GSIC presents a better tradeoff than GZF with the equal group-size partition {2,2,2,2}. This is explained by the successive reduction of the number of interferers for each group with GSIC. Surprisingly, performance with {3,2,2,1} does not provide the same conclusions. As indicated in the figure, GSIC does not outperform GZF when $r \in [r^{(2)}(\{3,2,2,1\}), r^{(3)}(\{3,2,2,1\})]$. This is explained by the fact that GSIC is performed with two active groups in that range of multiplexing rate, while GZF is still performed with only one group.

Next, we illustrate the optimization process with GZF when $G = 4$. The tradeoff with optimal-rate allocation for all possible partitions is evaluated and shown in Fig. 7. Clearly, {5,1,1,1} outperforms all other partitions for all ranges of r.

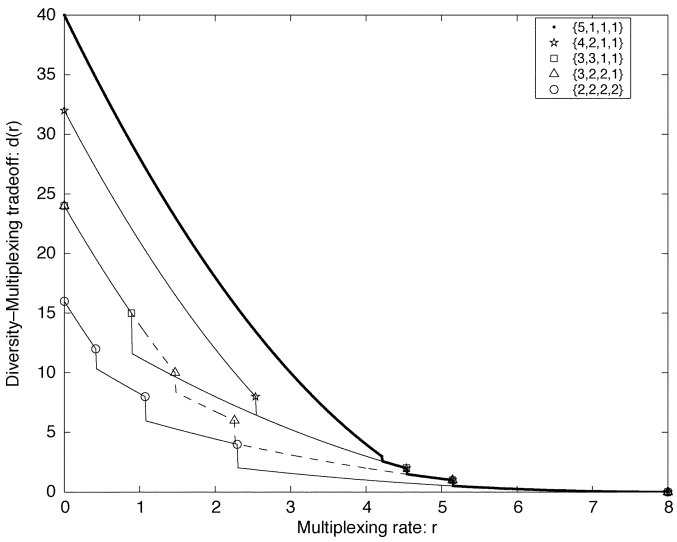

Fig. 7. Optimization of the GZF tradeoff with optimum-rate allocation. $N = K = 8$ and $G = 4$.

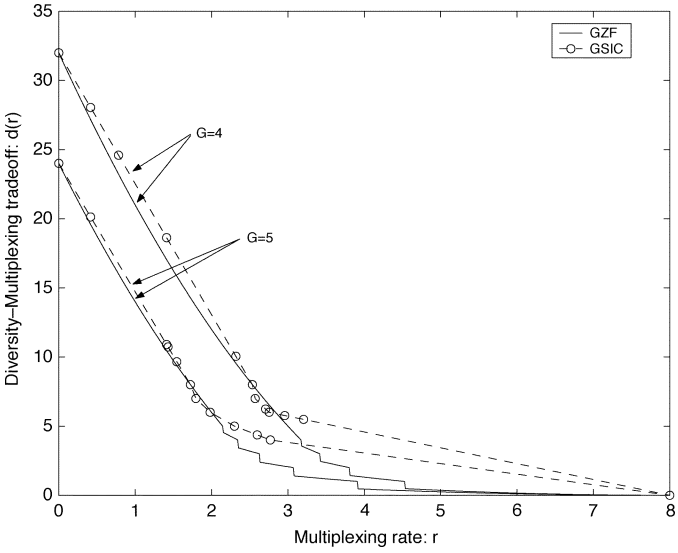

Fig. 8. Optimized tradeoff performance of GSIC and GZF with optimum-rate allocation. $N = K = 8$ and $G = 4$ and 5.

The optimized-tradeoff function with optimal-rate allocation is then obtained with {5,1,1,1}. Such a partition is indeed $\{p^*, G\}$, as found in Section V-C. As for the GSIC receiver, a similar process is performed, and maximization over all possible $(r^{(j)}, d_{\text{OptRate}}^{\text{GSIC},\{p,G\}}(j))$ for each partition provides a linearly approximated optimized tradeoff function. Fig. 8 puts forward an example of results when $G = 4$ and $G = 5$. First, we note that in contrast to the equal-rate and proportional-rate schemes (see Fig. 7), GZF and GSIC perform very closely to each other for low values of r. When $G = 4$, GZF even outperforms the GSIC receiver for $r \in [2.5, 3]$. The fact that the number of active groups with GSIC is larger than the one with GZF explains such results. At high values of r, $r > 3$ sym/s, GSIC presents a better tradeoff than GZF clearly for each $(r^{(j)}, d_{\text{OptRate}}^{\text{GSIC},\{p,G\}}(j))$. This implies that GZF should be used instead of GSIC for low values of r, since it provides the same level of performance with lower levels of computational

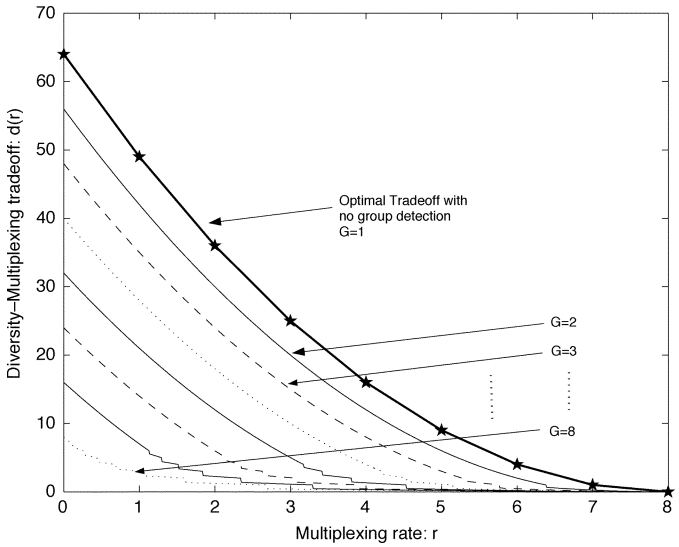

Fig. 9. Effect of G on the optimized tradeoff with optimal-rate allocation for GZF. $N = K = 8$ and $G = 2, 3, \ldots, 8$.

complexity. We have also compared the optimized performance of the optimal tradeoff with the size-proportional scheme for different values of G, and found that they perform very closely to each other at high multiplexing rates. Hence, the size-proportional rate-allocation scheme with GSIC might be deployed at high values of r to provide lower complexity levels. Results in this case are not shown in this paper, due to space limitations.

Finally, we investigate the effect of the number of groups on the optimized tradeoff of GZF with the optimal rate-allocation scheme. Fig. 9 provides the obtained results with GZF for $G = 2, \ldots, 8$. The optimal tradeoff with no group detection [2] is also shown for comparison. As in the case of the equal-rate and size-proportional rate-allocation schemes, the optimized tradeoff is enhanced when G is decreased. Indeed, when $G = 2$, GZF significantly approaches the optimal tradeoff, while $G = 8$ (V-BLAST) presents the worst performance, as found in Section V-C. As a result, we conclude that group detection can significantly bridge the gap between V-BLAST [6] and the optimal scheme [2], while offering low levels of complexity.

VII. Conclusions

In this paper, we considered a MIMO system where group detection is used at the receiver. For each of the groups, we evaluated its diversity-multiplexing tradeoff with both GZF and GSIC. We provided an expression of the overall system-outage probability as a function of the group outage ones, and showed that the overall system tradeoff is given by the worst group tradeoff performance. Several rate-allocation schemes have been proposed; namely, the equal rate, the size-proportional rate, and the optimal rate-allocation schemes. A closed-form expression of the tradeoff function with the latter scheme for the GZF receiver has been derived. Simulation results demonstrated that the size-proportional scheme outperforms the equal-rate one, and approaches the optimal one for high values of multiplexing rates. Moreover, when the tradeoff with optimal-rate allocation is optimized over all possible partitions for a given G, GZF performs close to the GSIC receiver for

a wide range of low values of r, and sometimes outperforms it. As a result, GZF can prove to be an alternative receiver to GSIC, providing similar levels of tradeoffs with much lower complexity. Finally, both GSIC and GZF have been shown to efficiently bridge the gap between the optimal performance [2] and BLAST, while decreasing G.

APPENDIX A
JOINT DISTRIBUTION OF Q_g^{-1} EIGENVALUES

Let us write $\boldsymbol{H}$ as $\boldsymbol{H} = [\boldsymbol{H}_g \ \boldsymbol{H}_{\overline{g}}]$, where $\overline{g}$ denotes the set of groups interfering with the gth group. According to [15], we have

$$\boldsymbol{Q}_g^{-1} = \boldsymbol{H}_g^{\dagger}\boldsymbol{P}_g\boldsymbol{H}_g$$

where $\boldsymbol{P}_g$ is a $N \times N$ projection matrix, such that

$$\boldsymbol{P}_g = \boldsymbol{I}_N - \boldsymbol{H}_{\overline{g}}\left(\boldsymbol{H}_{\overline{g}}^{\dagger}\boldsymbol{H}_{\overline{g}}\right)^{-1}\boldsymbol{H}_{\overline{g}}^{\dagger}. \tag{A.1}$$

Since the columns of $\boldsymbol{H}$ are independent of each other, then so are the columns of $\boldsymbol{H}_g$ and $\boldsymbol{H}_{\overline{g}}$. According to (A.1), $\boldsymbol{P}_g$ is expressed as a function of $\boldsymbol{H}_{\overline{g}}$ only. Hence, $\boldsymbol{P}_g$ is independent of $\boldsymbol{H}_g$. Moreover, $\boldsymbol{P}_g$ has $N - |\overline{g}|$ unit eigenvalues and $|\overline{g}|$ zero eigenvalues [14]–[15]. Let $\boldsymbol{P}_g$ be diagonalized [16] such that

$$\boldsymbol{P}_g = \boldsymbol{\Phi}_g^{\dagger}\boldsymbol{\Upsilon}_g\boldsymbol{\Phi}_g \tag{A.2}$$

where Φ_g is a unitary $N \times N$ matrix, and $\Upsilon_g = \mathrm{diag}(\gamma_1, \gamma_2, \ldots, \gamma_N)$, where $\{\gamma_1, \gamma_2, \ldots, \gamma_N\}$ are the ordered eigenvalues of $\boldsymbol{P}_g$. We can then write the following:

$$\boldsymbol{Q}_g^{-1} = \boldsymbol{H}_g^{\dagger}\boldsymbol{\Phi}_g^{\dagger}\boldsymbol{\Upsilon}_g\boldsymbol{\Phi}_g\boldsymbol{H}_g = \boldsymbol{Z}_g\boldsymbol{\Upsilon}_g\boldsymbol{Z}_g^{\dagger} \tag{A.3}$$

where $\boldsymbol{Z}_g = \boldsymbol{H}_g^{\dagger}\boldsymbol{\Phi}_g^{\dagger}$. Next, let $\boldsymbol{Z}_g$ be written as $\boldsymbol{Z}_g = [\boldsymbol{z}_1, \boldsymbol{z}_2, \ldots, \boldsymbol{z}_N]$. It follows that:

$$\boldsymbol{Q}_g^{-1} = \sum_{i=1}^{N}\gamma_i\boldsymbol{z}_i\boldsymbol{z}_i^{\dagger} = \sum_{i=1}^{N-|\overline{g}|}\boldsymbol{z}_i\boldsymbol{z}_i^{\dagger}. \tag{A.4}$$

Since $\boldsymbol{\Phi}_g$ is a unitary matrix, so is $\boldsymbol{\Phi}_g^{\dagger}$. Consequently, $\boldsymbol{Z}_g$ has the same distribution as $\boldsymbol{H}_g^{\dagger}$, and $\{z_1, z_2, \ldots, z_N\}$, conditioned on $\boldsymbol{\Phi}_g$, are complex Gaussian-distributed $|g|$-length vectors with zero mean and covariance $\boldsymbol{I}_{|g|}$. Hence, conditioned on $\{\gamma_1, \gamma_2, \ldots, \gamma_N\}$, $\boldsymbol{Q}_g^{-1}$ is Wishart distributed with $N - |\overline{g}|$ degrees of freedom, denoted by $\mathcal{W}_{|g|}(N - |\overline{g}|, \boldsymbol{I}_{|g|})$ [17]. However, since $\{\gamma_1, \gamma_2, \ldots, \gamma_N\}$ are either "1" or "0," and are independent of $\boldsymbol{H}_g$, $\boldsymbol{Q}_g^{-1}$ is $\mathcal{W}_{|g|}(N - |\overline{g}|, \boldsymbol{I}_{|g|})$ and has $|g|$ eigenvalues. Let $\{\mu_1, \mu_2, \ldots, \mu_{|g|}\}$ be these eigenvalues in the ascending order. According to [17], $\{\mu_1, \mu_2, \ldots, \mu_{|g|}\}$ are distributed as in (17). Finally, we note that when real constellations are used, the results are changed, according to [15].

APPENDIX B

A. Optimal Ordering for Equal-Rate Allocation

Without loss of generality, consider the two orders $\{g_1, \ldots, g_i, \ldots, g_k, \ldots g_G\}$ and $\{g_1, \ldots, g_k, \ldots, g_i, \ldots g_G\}$, where the ith and kth positions, with $i < k$, are interchanged. Consider the gth retrieved group with both orders. Denote by $|\overline{g}^1|$ and $|\overline{g}^2|$ the sizes of its interferers, and by $d_g^1(r)$ and $d_g^2(r)$ its corresponding tradeoff, respectively. According to (19), we have $|\overline{g}^1| = |\overline{g}^2|$ and $d_g^1(r) = d_g^2(r)\ \forall g \in \{1, \ldots, i-1, k+1, \ldots, G\}$. However, when $g \in \{i, \ldots, k\}$, $|\overline{g}^1| = \sum_{\substack{l=g+1 \\ l\neq k}}^{G}|g_l| + |g_k|$ and $|\overline{g}^2| = \sum_{\substack{l=g+1 \\ l\neq k}}^{G}|g_l| + |g_i|$. Since $i \leq k$, $|g_i| \geq |g_k|$ and $|\overline{g}^1| < |\overline{g}^2|$, implying that $d_g^1(r) \geq d_g^2(r)$. It follows that $\min_{g=1,\ldots,G}\{d_g^1(r)\} \geq \min_{g=1,\ldots,G}\{d_g^2(r)\}$ and that the first ordering outperforms the second one. Therefore, we conclude that the tradeoff function of GSIC with equal-rate control is maximized when the groups are retrieved in the decreasing order of their size.

B. Derivation of $d_{\mathrm{OptRate}}^{\mathrm{GZF},\{p,G\}}(j)$ for GZF With Optimal-Rate Control

Consider the partition $\{p, G\} = \{g_1, g_2, \ldots, g_G\}$, and let $\{g(1), g(2), \ldots, g(j+1)\}$ be a random subset of $\{p, G\}$ consisting of $(j+1)$ groups, such that $|g(1)| \geq |g(2)| \geq \ldots \geq |g(j+1)|$. Let $d_{g(i)}^{\mathrm{GZF}}(r_{g(i)})$ denote the tradeoff of each of these groups. According to (18), we have $\min_{i=1,\ldots,j+1}\{d_{g(i)}^{\mathrm{GZF}}(r_{g(i)})\} = (N - K_{j+1} + |g(j+1)|)\,|g(j+1)|$ with $K_{j+1} = \sum_{i=1}^{j}|g(i)|$. Assuming that $\{g(1), g(2), \ldots, g(j)\}$ are already chosen, $\min_{i=1,\ldots,j+1}\{d_{g(i)}^{\mathrm{GZF}}(r_{g(i)})\}$ is maximized when $|g(j+1)|$ is maximized. Since $|g(j+1)| = \min_{i=1,\ldots,j+1}\{|g(i)|\}$, $g(j+1) = g_{j+1}$ and $\{g(1), g(2), \ldots, g(j+1)\} = \{g_1, g_2, \ldots, g_G\}$. $d_{\mathrm{OptRate}}^{\mathrm{GZF},\{p,G\}}(j)$ then follows immediately.

C. Derivation of $r^{(j)}$ for GZF With Optimal-Rate Control

Let $\{r_{g_1}^{(j)}, r_{g_2}^{(j)}, \ldots, r_{g_j}^{(j)}\}$ be the multiplexing rate allocated to $\{g_1, g_2, \ldots, g_j\}$ when $r = r^{(j)}$, then $r^{(j)} = \sum_{i=1}^{j} r_{g_i}^{(j)}$. We evaluate in what follows $\{r_{g_1}^{(j)}, r_{g_2}^{(j)}, \ldots, r_{g_j}^{(j)}\}$. Consider $i \in \{1, \ldots, j\}$, then $r_{g_i}^{(j)}$ satisfies

$$\left(N - K^{(j)} + |g_i| - r_{g_i}^{(j)}\right)\left(|g_i| - r_{g_i}^{(j)}\right) = \left(N - K^{(j)}\right)|g_{j+1}|. \tag{B.2}$$

Let $X_i = |g_i| - r_{g_i}^{(j)}$. According to the notations in (12), (B.2) is equivalent to $(A^{(j)} - X_i)X_i = A^{(j)}|g_{j+1}|$ or

$$(X_i)^2 + A^{(j)}X_i - A^{(j)}|g_{j+1}| = 0. \tag{B.3}$$

Equation (B.3) admits $\Delta^{(j)} = (A^{(j)})^2 + 4A^{(j)}|g_{j+1}|$, which is always positive, since $A^j \geq 0$. (B.3) has, then, two solutions given by $1/2[-A^{(j)} \pm \sqrt{\Delta^{(j)}}]$. Since $0 \leq X_i \leq |g_i|$, we have $X_i = 1/2[-A^{(j)} + \sqrt{\Delta^{(j)}}]$. Hence, $r_{g_i}^{(j)} = |g_i| - X_i$ and $r^{(j)} = Nj/2 + (1 - j/2)K^{(j)} - j/2\sqrt{\Delta^{(j)}}$.

D. Derivation of $\{r_{g_1}(j), r_{g_2}(j), \ldots, r_{g_j}(j)\}$ for GZF With Optimal-Rate Control

Assume that the system consists of j active groups only; namely, $\{g_1, g_2, \ldots, g_j\}$, and let $r \in [r^{(j-1)}, r^{(j)}]$. We derive in what follows $\{r_{g_1}(j), r_{g_2}(j), \ldots, r_{g_j}(j)\}$, the multiplexing rate

allocated to each of these groups, such that $\sum_{i=1}^{j} r_{g_i}(j) = r$ and

$$d_{g_i}^{\mathrm{GZF}}\left(r_{g_i}(j)\right) = d_{g_1}^{\mathrm{GZF}}\left(r_{g_1}(j)\right) \quad \forall i \in \{2,\ldots,j\}. \tag{B.4}$$

Consider $i \in \{2,\ldots,j\}$. According to (12), (B.4) is equivalent to

$$\begin{aligned}&\left(N - K^{(j)} + |g_i| - r_{g_i}(j)\right)\left(|g_i| - r_{g_i}(j)\right)\\ &\quad = \left(N - K^{(j)} + |g_1| - r_{g_1}(j)\right)\left(|g_1| - r_{g_1}(j)\right). \end{aligned}\tag{B.5}$$

Let $X_i = |g_i| - r_{g_i}(j)$. Then (B.5) is rewritten as

$$\left(A^{(j)} + X_i\right) X_i = \left(A^{(j)} + X_1\right) X_1. \tag{B.6}$$

It is easy to see that (B.6) has $X_i = X_1$ as the only possible solution, since $X_i \geq 0$. It follows that $r_{g_i}(j) = |g_i| - |g_1| + r_{g_1} j)$. Since $\sum_{i=1}^{j} r_{g_i}(j) = r$, (26) and (27) are obtained.

E. Optimality of $\{g_1, g_2, \ldots, g_j\}$ When $r \in [r^{(j-1)}, r^{(j)}]$ With GZF

We shall prove here that when $r \in [r^{(j-1)}, r^{(j)}]$, the diversity achieved with $\{g_1, g_2, \ldots, g_j\}$ is larger than the one achieved by any other partition of j groups out of $\{p, G\}$. Without loss of generality, we consider the set $\{g_k, g_2, \ldots, g_j\}$ with $k \in \{j+1, \ldots, G\}$. Let $d_{\mathrm{OptRate}}^{\mathrm{GZF}}(r)$ and $d_k(r)$ denote the diversity achieved with both partitions, respectively. Then, since (B.4) is satisfied with both partitions, it follows that

$$\begin{cases} d_{\mathrm{OptRate}}^{\mathrm{GZF}}(r) = \left(N - \sum_{l=2}^{j} |g_l| - r_{g_1}(j)\right)\left(|g_1| - r_{g_1}(j)\right) \\ d_k(r) = \left(N - \sum_{l=2}^{j} |g_l| - r_{g_k}(j)\right)\left(|g_i| - r_{g_k}(j)\right). \end{cases}$$

$r_{g_1}(j)$ and $r_{g_k}(j)$ are provided by (27) such that

$$\begin{cases} r_{g_1}(j) = \frac{1}{j}\left(r + j|g_1| - K^{(j)}\right) \\ r_{g_k}(j) = \frac{1}{j}\left(r + j|g_k| - \left(K^{(j)} - |g_1| + |g_k|\right)\right). \end{cases}$$

By comparing $r_{g_1}(j)$ and $r_{g_k}(j)$, we find that $r_{g_1}(j) - r_{g_k}(j) = (|g_1| - |g_k|)(1 - (1/j))$, which is strictly positive for $1 < j < G$. We also obtain that $|g_1| - r_{g_1}(j) > |g_k| - r_{g_k}(j)$. It follows that $d_{\mathrm{OptRate}}^{\mathrm{GZF}}(r) > d_k(r)$ when $1 < j < G$. When $j = 1$, we have $r_{g_1}(j) = r_{g_k}(j) = r$, and $d_{\mathrm{OptRate}}^{\mathrm{GZF}}(r) > d_k(r)$.

REFERENCES

[1] R. D. Murch and K. B. Letaief, "Antenna systems for broadband wireless access," *IEEE Commun. Mag.*, vol. 40, no. 4, pp. 76–83, Apr. 2002.

[2] L. Zheng and D. N. Tse, "Diversity and multiplexing: A fundamental tradeoff in multiple antenna channels," *IEEE Trans. Inf. Theory*, vol. 49, no. 5, pp. 1073–1096, May 2003.

[3] V. Tarokh, N. Seshadri, and A. R. Calderbank, "Space–time codes for high data rate wireless communication: Performance criterion and code construction," *IEEE Trans. Inf. Theory*, vol. 44, no. 2, pp. 744–765, Mar. 1998.

[4] V. Tarokh, H. Jafarkhani, and A. R. Calderbank, "Space–time block codes from orthogonal designs," *IEEE Trans. Inf. Theory*, vol. 45, no. 5, pp. 1456–1467, May 1999.

[5] S. M. Alamouti, "A simple transmit diversity technique for wireless communications," *IEEE J. Sel. Areas. Commun.*, vol. 16, no. 8, pp. 1451–1458, Oct. 1998.

[6] S. Sandhu and A. Paulraj, "Space–time block codes: A capacity perspective," *IEEE Commun. Lett.*, vol. 4, no. 12, pp. 384–386, Dec. 2000.

[7] B. Hassibi and B. M. Hochwald, "High-rate codes that are linear in space and time," *IEEE Trans. Inf. Theory*, vol. 48, no. 7, pp. 1804–1824, Jul. 2002.

[8] G. J. Foschini, G. D. Golden, R. A. Valenzuela, and P. W. Wolniansky, "Simplified processing for high spectral efficiency wireless communication employing multi-element arrays," *IEEE J. Sel. Areas. Commun.*, vol. 17, no. 11, pp. 1841–1852, Nov. 1999.

[9] E. Telatar, "Capacity of multi-antenna Gaussian channels," *AT&T Bell Labs Internal Tech. Memo.*, Jun. 1995.

[10] V. Tarokh, A. Naguib, N. Seshadri, and A. R. Calderbank, "Combined array processing and space–time coding," *IEEE Trans. Inf. Theory*, vol. 45, no. 4, pp. 1121–1128, May 1999.

[11] N. Prasad and M. K. Varanasi, "Optimum efficiently decodable layered space–time block codes," in *Proc. IEEE 35th Asilomar Conf. Signals, Syst., Computers*, vol. 1, Nov. 2001, pp. 227–231.

[12] S. Sfar and K. B. Letaief, "Group ordered successive interference cancellation for multiuser detection in MIMO CDMA systems," in *Proc. IEEE Wireless Commun. Netw. Conf.*, vol. 2, Mar. 2003, pp. 888–893.

[13] M. K. Varanasi, "Group detection for synchronous Gaussian code-division multiple-access channels," *IEEE Trans. Inf. Theory*, vol. 41, no. 4, pp. 1083–1096, Jul. 1995.

[14] M. K. Varanasi, "Decision feedback multiuser detection: A systematic approach," *IEEE Trans. Inf. Theory*, vol. 45, no. 1, pp. 219–240, Jan. 1999.

[15] S. Sfar and K. B. Letaief, "Improved group multiuser detection with multiple antennas in the presence of improper multiaccess interference," *IEEE Trans. Commun.*, vol. 53, no. 4, pp. 560–563, Apr. 2005.

[16] R. A. Horn and C. R. Johnson, *Matrix Analysis*. Cambridge, U.K.: Cambridge Univ. Press, 1990.

[17] R. K. Mallik, "The pseudo-Wishart distribution and its application to MIMO systems," *IEEE Trans. Inf. Theory*, vol. 49, no. 10, pp. 2761–2769, Oct. 2003.

Sana Sfar (S'01–A'05) is currently working toward the Ph.D. degree in electrical and electronic engineering at the Hong Kong University of Science and Technology (HKUST), Kowloon, with focus on wireless communications. She received the MPhil. degree in 2001 from the same school, and the Engineering Diploma in telecommunications (with Excellence) in 1999 from the École Supérieure des Communications de Tunis, Tunis, Tunisia, with focus on multimedia and networking.

Her current research interests are in the area of wireless communication systems and communication theory. These include wireless and mobile networks, broadband wireless access, MIMO techniques, space–time coding, channel coding and modulation, OFDM, CDMA, and Beyond 3G systems. In these areas, she has published over 17 journal and conference papers.

Ms. Sfar has served as Session Chair for ICC 2001, Helsinki. She also served as a reviewer for numerous IEEE journals and conferences, including IEEE TRANSACTIONS ON COMMUNICATIONS, IEEE TRANSACTIONS ON SIGNAL PROCESSING, IEEE JOURNAL OF SELECTED AREAS IN COMMUNICATIONS, IEEE TRANSACTIONS ON VEHICULAR TECHNOLOGY, and the *EURASIP Journal on Applied Signal Processing*. She has received numerous awards throughout her studies, including the IEEE Communications Society Student Travel Grant Award in 2001, 2003, and 2004; the Tunisian National Postgraduate Fellowship Award in 1999, and the Tunisie Telecom Excellence Grant in 1999. She was also a National Laureate in the Baccalaureate Examination of 1994, and ranked in the top 3% of the overall admitted national candidates.

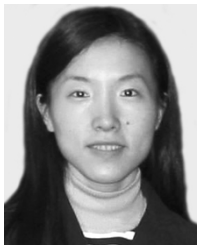

Lin Dai (S'00–M'03) was born in Wuhan, China, in 1979. She received the B.S. degree in electronic engineering from Huazhong University of Science and Technology, Wuhan, China, in 1998, and the M.S. and Ph.D. degrees in electrical and electronic engineering from Tsinghua University, Beijing, China, in 2000 and 2002, respectively.

She was with Alcatel Shanghai Bell Co., Ltd. as a Visiting Researcher and worked on the design and implementation of a WCDMA commercial prototype from April to July, 2001. Since 2003, she has been with the Hong Kong University of Science and Technology, Hong Kong, where she is a Postdoctoral Fellow. Her research interests include wireless communications, and information and communication theory.

Khaled Ben Letaief (S'85–M'86–SM'97–F'03) received the B.S. degree *with distinction* in 1984, and the M.S. and Ph.D. degrees in 1986 and 1990, respectively, all in electrical engineering, from Purdue University, West Lafayette, IN.

From January 1985 and as a Graduate Instructor in the School of Electrical Engineering at Purdue University, he taught courses in communications and electronics. From 1990 to 1993, he was a Faculty Member with the University of Melbourne, Melbourne, Australia. Since 1993, he has been with the Hong Kong University of Science and Technology, Kowloon, where he is currently Professor and Head of the Electrical and Electronic Engineering Department. He is also the Director of the Hong Kong Telecom Institute of Information Technology, as well as the Director of the Center for Wireless Information Technology. His current research interests include wireless and mobile networks, broadband wireless access, OFDM, CDMA, and Beyond 3G systems. In these areas, he has published over 270 journal and conference papers and given invited talks as well as courses all over the world. He has served as consultant for different organizations, as well.

Dr. Letaief is the founding Editor-in-Chief of the IEEE TRANSACTIONS ON WIRELESS COMMUNICATIONS. He has served on the editorial board of other prestigious journals, including the IEEE JOURNAL ON SELECTED AREAS IN COMMUNICATIONS—WIRELESS SERIES (as Editor-in-Chief) and the IEEE TRANSACTIONS ON COMMUNICATIONS. He has been involved in organizing a number of major international conferences and events. These include serving as the Technical Program Chair of the 1998 IEEE Globecom Mini-Conference on Communications Theory, as well as the Co-Chair of the 2001 IEEE ICC Communications Theory Symposium. In 2004, he served as the Co-Chair of the IEEE Wireless Communications, Networks and Systems Symposium, as well as the Co-Technical Program Chair of the 2004 IEEE International Conference on Communications, Circuits and Systems. He served as the Chair of the IEEE Communications Society Technical Committee on Personal Communications, and is a member of the IEEE ComSoc Technical Activity Council. He received the Mangoon Teaching Award from Purdue University in 1990; the Teaching Excellence Appreciation Award from the School of Engineering at HKUST (four times); and the Michael G. Gale Medal for Distinguished Teaching (highest university-wide teaching award and only one recipient/year is honored for his/her contributions). He is an IEEE Distinguished Lecturer of the IEEE Communications Society.